Reductive Elimination of *cis*-PtMe(SiPh$_3$)(PMePh$_2$)$_2$

Fumiyuki Ozawa,* Toshihiko Hikida, and Tamio Hayashi*

Contribution from the Catalysis Research Center and Graduate School of Pharmaceutical Sciences, Hokkaido University, Kita-ku, Sapporo 060, Japan

*Received December 2, 1993**

Abstract: Novel *cis*- and *trans*-(silyl)(methyl)platinum(II) complexes were prepared and their reactivity toward reductive elimination was examined. Treatment of *trans*-PtCl(SiPh$_3$)(PMePh$_2$)$_2$ (**1**) with an excess amount of MeLi in THF followed by methanolysis of the reaction system gave *cis*-PtMe(SiPh$_3$)(PMePh$_2$)$_2$ (**2**), selectively. On the other hand, reaction of **1** with Me$_2$Mg in THF formed *trans*-PtMe(SiPh$_3$)(PMePh$_2$)$_2$ (**3**). The structure of *cis*-**2** was determined by X-ray diffraction study. Crystal data for *cis*-**2**·Et$_2$O: monoclinic, space group $P2_1/c$, $a = 16.113(3)$ Å, $b = 11.354(3)$ Å, $c = 25.216(2)$ Å, $\beta = 104.73(1)°$, $V = 4461(1)$ Å^3, $Z = 4$, $d_{calcd} = 1.405$ g cm^{-3}, $R = 0.038$, $R_w = 0.033$, $S = 1.72$. Thermolysis of **2** and **3** readily proceeded in a benzene solution to yield quantitative amounts of MeSiPh$_3$ as the reductive elimination product. Kinetic studies on the thermolysis of *cis*-**2** revealed that the reductive elimination is predominantly initiated by dissociation of the PMePh$_2$ ligand and accelerated by acetylenes and olefins added to the system.

Introduction

Hydrosilylation of olefins catalyzed by transition metal complexes is a versatile synthetic means of organosilicon compounds.[1] This reaction is generally assumed to proceed by the Chalk–Harrod mechanism (Scheme 1).[2] Oxidative addition of hydrosilane to a low valent transition metal complex (**A**) gives a hydrido–silyl complex (**B**), which subsequently undergoes olefin-insertion into the metal–hydride bond to give an alkyl–silyl species (**C**). Reductive elimination of the alkyl and silyl ligands from **C** forms the hydrosilylation product.

Although the Chalk–Harrod mechanism has accounted for a number of observations associated with catalytic hydrosilylation, direct support for the mechanism based on the studies of isolated transition metal silyl complexes is still lacking. Particularly, there is only one example for reductive elimination of an isolated silyl–alkyl complex reported[3] and an alternative mechanism without reductive elimination of silyl–alkyl species **C** has been recently proposed.[4]

One of the most common catalysts for hydrosilylation is a platinum complex.[1] It is well documented that organoplatinum complexes are extremely stable toward reductive elimination.[5] Furthermore, recent theoretical studies showed that the Pt–Si bond is much stronger than the Pt–C bond.[6] These data may be taken as an indication that the reductive elimination of (silyl)-(alkyl)platinum species is a difficult process,[7] while the reductive elimination of such species is essential for the Chalk–Harrod mechanism to be operative.

Scheme 1

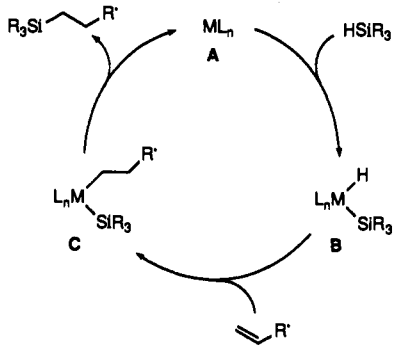

Scheme 2

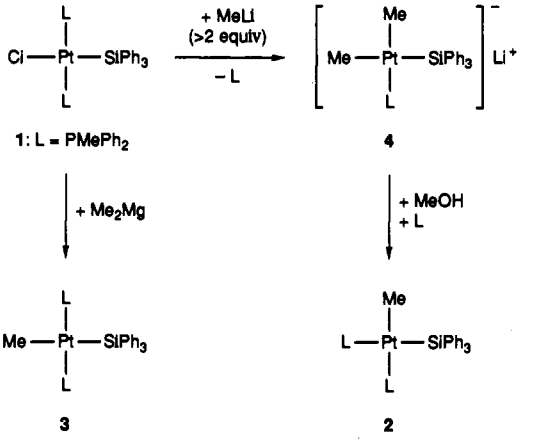

In order to explore these important problems concerning the hydrosilylation mechanism, we prepared in this study well-characterized (silyl)(alkyl)platinum complexes *cis*- and *trans*-PtMe(SiPh$_3$)(PMePh$_2$)$_2$ (**2** and **3**, respectively) and examined their reactivity toward reductive elimination. Kinetic studies revealed that *cis*-**2** possesses unexpectedly high reactivity toward reductive elimination.

Results and Discussion

Stereoselective Synthesis of *cis*- and *trans*-PtMe(SiPh$_3$)-(PMePh$_2$)$_2$. It has been well documented that reductive elim-

* Abstract published in *Advance ACS Abstracts,* March 1, 1994.

(1) (a) Ojima, I. In *The Chemistry of Organic Silicon Compounds*; Patai, S., Rappoport, Z., Eds.; John Wiley: Chichester, 1989; p 1479. (b) Speier, J. L. *Advanced Organometallic Chemistry*; Stone, F. G. A., West, R., Eds.; Academic Press: New York, 1979; Vol. 17, p 407. (c) Lukevics, E.; Belyakova, Z. V.; Pomerantseva, M. G.; Voronkov, M. G. In *Journal of Organometallic Chemistry Library*; Seyferth, D., Davies, A. G., Fisher, E. O., Normant, J. F., Reutov, O. A., Eds.; Elsevier: Amsterdam, 1977; Vol. 5. (d) Ojima, I.; Kogure, T. *Rev. Silicon, Germanium, Tin Lead Compd.* **1981**, *5*, 7.

(2) (a) Chalk, A. J.; Harrod, J. F. *J. Am. Chem. Soc.* **1965**, *87*, 16. (b) Tilley, T. D. In *The Chemistry of Organic Silicon Compounds*; Patai, S., Rappoport, Z., Eds.; John Wiley: Chichester, 1989; p 1415.

(3) Brinkman, K. C.; Blakeney, A. J.; Krone-Schmidt, W.; Gladysz, J. A. *Organometallics* **1984**, *3*, 1325. Blakeney, A. J.; Gladysz, J. A. *Inorg. Chim. Acta Lett.* **1981**, *53*, L25.

(4) (a) Bergens, S. H.; Noheda, P.; Whelan, J.; Bosnich, B. *J. Am. Chem. Soc.* **1992**, *114*, 2128. (b) Duckett, S.; Pertsz, R. N. *Organometallics* **1992**, *11*, 90. For a recent mechanistic study of platinum-catalyzed hydrosilylation of olefins, see: Lewis, L. N. *J. Am. Chem. Soc.* **1990**, *112*, 5998.

(5) Low, J. J.; Goddard, W. A., III *J. Am. Chem. Soc.* **1986**, *108*, 6115 and references cited therein.

(6) (a) Sakaki, S.; Ieki, M. *J. Am. Chem. Soc.* **1991**, *113*, 5063. (b) Sakaki, S.; Ieki, M. *J. Am. Chem. Soc.* **1993**, *115*, 2373.

(7) A theoretical study predicted that reductive elimination of cis-Pt(CH$_3$)-(SiH$_3$)(PH$_3$)$_2$ requires the activation energy of 39 kcal/mol.[6b]

0002-7863/94/1516-2844$04.50/0

Table 1. NMR Data for *cis*- and *trans*-PtMe(SiPh$_3$)(PMePh$_2$)$_2$ (**2** and **3**)[a]

	^{1}H NMR				^{31}P{^{1}H} NMR				
complex	δ	J_{H-P}	J_{H-Pt}	assignment	δ	J_{P-P}	J_{P-Pt}	J_{P-Si}	assignment
cis-**2**	0.15 (dd)	12.5, 6.3	57.1	PtMe	11.6 (d)	18	1387	190	P(1)
	1.26 (d)	6.9	14.6	PMe	6.4 (d)	18	2136	0	P(2)
	1.34 (d)	7.9	28.0	PMe					
trans-**3**	−0.55 (t)	6.9	43.6	PtMe	12.6 (s)		2886	0	
	1.48 (vt)[b]	3.0[c]	35.6	PMe					

[a] In CD_2Cl_2, at −20 °C. Chemical shifts are reported in δ ppm and coupling constants in Hz. [b] vt: virtual triplet. [c] Apparent coupling constant for the virtual triplet signal.

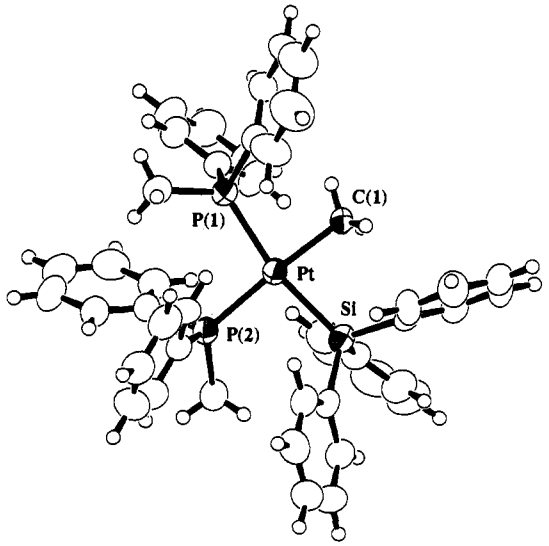

Figure 1. Molecular structure of *cis*-PtMe(SiPh$_3$)(PMePh$_2$)$_2$·Et$_2$O (**2**). The Et$_2$O molecule is omitted for simplicity. Selected bond distances (Å) and angles (deg): Pt–C(1) = 2.113(7), Pt–Si = 2.381(2), Pt–P(1) = 2.361(2), Pt–P(2) = 2.293(2); Si–Pt–C(1) = 82.2(2), P(1)–Pt–P(2) = 98.02(7), P(1)–Pt–Si = 167.34(7), P(1)–Pt–C(1) = 85.2(2), P(2)–Pt–Si = 94.53(7), P(2)–Pt–C(1) = 175.0(2).

ination of diorgano complexes of d^8 metals in MRR′L$_2$ takes places only from the cis isomer by a concerted process involving a three-centered transition state and reductive elimination of the trans isomer requires its prior isomerization to the cis isomer.[8] Therefore, we first examined stereoselective synthesis of the two geometrical isomers of (silyl)(methyl)platinum(II) complexes *cis*- and *trans*-PtMe(SiPh$_3$)(PMePh$_2$)$_2$ (**2** and **3**, respectively) (Scheme 2). The cis isomer **2** could be prepared by the use of an anionic platinum dimethyl(silyl) intermediate **4**.[9] Treatment of *trans*-PtCl(SiPh$_3$)(PMePh$_2$)$_2$ (**1**)[10] with an excess amount of MeLi in THF at room temperature gave **4** with liberation of 1 equiv of PMePh$_2$. The subsequent treatment of the reaction system with methanol resulted in selective protonation at the methyl ligand trans to the silyl group in **4** to give the *cis*-(silyl)(methyl) complex **2**. On the other hand, reaction of **1** with Me$_2$Mg exclusively formed *trans*-**3**.

The anionic intermediate **4** was not isolated but its formation in the reaction system was clearly observed by NMR spectroscopy. In the ^{31}P{^{1}H} NMR spectrum, the starting silyl–chlorido complex **1** exhibited a singlet at δ 11.1 ($^1J_{P-Pt}$ = 2909 Hz). When MeLi (3 equiv) was added to a THF-d_8 solution of **1**, the singlet at δ 11.1 instantly disappeared and a new singlet assignable to **4** (δ 11.8, $^1J_{P-Pt}$ = 2039 Hz) and a broad signal (δ −26.2) arising from free PMePh$_2$ appeared in a 1:1 ratio. Addition of methanol to the reaction mixture resulted in selective formation of *cis*-**2** at the expense of **4** and free PMePh$_2$.[11] ^{1}H NMR data of **4** also supported the dimethyl(silyl)platinate structure.[12]

Complexes *cis*-**2** and *trans*-**3** thus prepared were isolated as colorless crystals and identified by elemental analysis and NMR spectroscopy. Table 1 lists the NMR data of *cis*-**2** and *trans*-**3**. The ^{31}P{^{1}H} NMR of *trans*-**3** exhibited a singlet signal with relatively large coupling to the ^{195}Pt nucleus ($^1J_{P-Pt}$ = 2886 Hz), the value being in the typical range for a *trans*-bis(tertiary phosphine)platinum(II) complex.[13] In the ^{31}P{^{1}H} NMR of *cis*-**2**, on the other hand, the two phosphorus nuclei (P(1) and P(2)) were observed as nonequivalent doublets at δ 11.6 and 6.4, respectively ($^2J_{P(1)-P(2)}$ = 18 Hz). The doublet observed at lower magnetic field (P(1)) exhibited satellite signals arising from the coupling to the ^{29}Si nucleus ($^2J_{P(1)-Si}$ = 190 Hz), whereas the other doublet at higher magnetic field showed no coupling toward the silyl nucleus. Hence the P(1) and P(2) signals are assigned to the phosphine ligands trans and cis to the Ph$_3$Si ligand, respectively. It was noted that the $^1J_{P-Pt}$ value of the P(1) signal (1387 Hz) is significantly smaller than that of the P(2) signal (2136 Hz), indicating the greater trans influence of the silyl ligand than the methyl ligand.[14]

X-ray Structure of *cis*-2. The greater trans influence of the Ph$_3$Si ligand than the methyl ligand was also confirmed by X-ray diffraction study of *cis*-**2**. As seen from the X-ray structure in Figure 1, the Pt–P(1) bond (2.361(2) Å), which is situated trans to the Ph$_3$Si ligand, was significantly longer than the Pt–P(2) bond (2.293(2) Å) at the site trans to the methyl ligand. The Pt–P(2) distance is similar to the Pt–P distances in *cis*-PtMe$_2$(PMePh$_2$)$_2$ (2.285 and 2.284 Å).[15] The Si–Pt–C(1) angle (82.2(2)°) is slightly wider than the Me–Pt–Me angle in *cis*-PtMe$_2$(PMePh$_2$)$_2$ (81.9°).

Site Selective Ligand Displacement of *cis*-2 with PMe$_2$Ph. Owing to the great trans labilizing effect of the silyl ligand, the PMePh$_2$ ligand trans to the silyl ligand in *cis*-**2** is readily replaced by other ligands. Figure 2 shows the change in ^{31}P{^{1}H} NMR spectra in the reaction of *cis*-**2** with 1.5 equiv of PMe$_2$Ph in CD_2Cl_2 at −20 °C. Figure 2a represents the spectrum of pure *cis*-**2**. On addition of PMe$_2$Ph to the solution, the signals arising from *cis*-**2** instantly decreased their intensity, and a new set of signals assignable to PtMe(SiPh$_3$)(PMe$_2$Ph)(PMePh$_2$) (**5**) and free

(8) (a) Yamamoto, A. *Organotransition Metal Chemistry. Fundamental Concepts and Applications*; Wiley-Interscience: New York, 1986, p 240. (b) Crabtree, R. H. *The Organometallic Chemistry of the Transition Metals*; Wiley-Interscience: New York, 1988, p 132. (c) Collman, J. P.; Hegedus, L. S.; Norton, J. R.; Finke, R. G. *Principles and Applications of Organotransition Metal Chemistry*; University Science Books: Mill Valley, CA, 1987; p 323.

(9) Similar strategy of controlling square planar geometry was reported for palladium alkyl systems: (a) Ozawa, F.; Ito, T.; Nakamura, Y.; Yamamoto, A. *Bull. Chem. Soc. Jpn.* **1981**, *54*, 1868. (b) Nakazawa, H.; Ozawa, F.; Yamamoto, A. *Organometallics* **1983**, *2*, 241. (c) Ozawa, F.; Kurihara, K.; Fujimori, M.; Hidaka, T.; Toyoshima, T.; Yamamoto, A. *Organometallics* **1989**, *8*, 180.

(10) Chatt, J.; Eaborn, C.; Ibekwe, S. D.; Kapoor, P. N. *J. Chem. Soc.* (*A*) **1970**, 1343.

(11) The ^{31}P{^{1}H} NMR spectra showing the sequence of reactions (**1** → **4** → **2**) are given in the supplementary material.

(12) ^{1}H NMR data of **4** (THF-d_8): δ −0.26 (d, $^3J_{H-P}$ = 7.3 Hz, $^2J_{H-Pt}$ = 59.4 Hz, 3H, PtCH_3), 0.33 (d, $^3J_{H-P}$ = 7.3 Hz, $^2J_{H-Pt}$ = 68.6 Hz, 3H, PtCH_3), 1.23 (d, $^2J_{H-P}$ = 6.9 Hz, $^3J_{H-Pt}$ = 22.4 Hz, 3H, PCH_3), 6.7–7.6 (m, *Ar*).

(13) Pregosin, P. S.; Kunz, R. W. *^{31}P and ^{13}C NMR of Transition Metal Phosphine Complexes*; Springer-Verlag: Berlin, 1979.

(14) The $^1J_{Pt-P}$ value of the P(1) signal is smaller than those for *cis*-bis(silyl)- and *cis*-(hydrido)(silyl)bis(tertiary phosphine)platinum(II) complexes (ca. 1500 Hz): Yamashita, H.; Kobayashi, T.; Hayashi, T.; Tanaka, M. *Chem. Lett.* **1990**, 1447. Ciriano, M.; Green, M.; Howard, J. A. K.; Proud, J.; Spencer, J. L.; Stone, F. G. A. *J. Chem. Soc., Dalton Trans.* **1978**, 801.

(15) Ibers, J.; Bartczak, T.; Ibers, J. A.; Low, J. J.; Goddard, W. A., III *J. Am. Chem. Soc.* **1986**, *108*, 347.

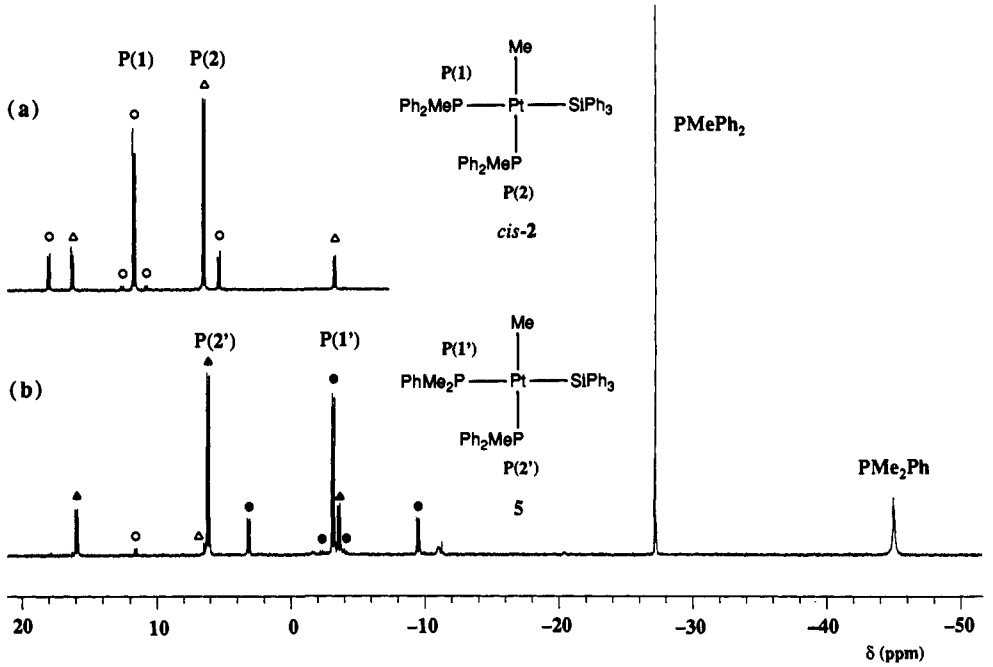

Figure 2. (a) $^{31}P\{^1H\}$ NMR spectrum (109.25 MHz) of *cis*-**2** in CD_2Cl_2 at −20 °C. (b) $^{31}P\{^1H\}$ NMR spectrum (109.25 MHz) of the reaction solution of *cis*-**2** with 1.5 equiv of PMe_2Ph in CD_2Cl_2 at −20 °C.

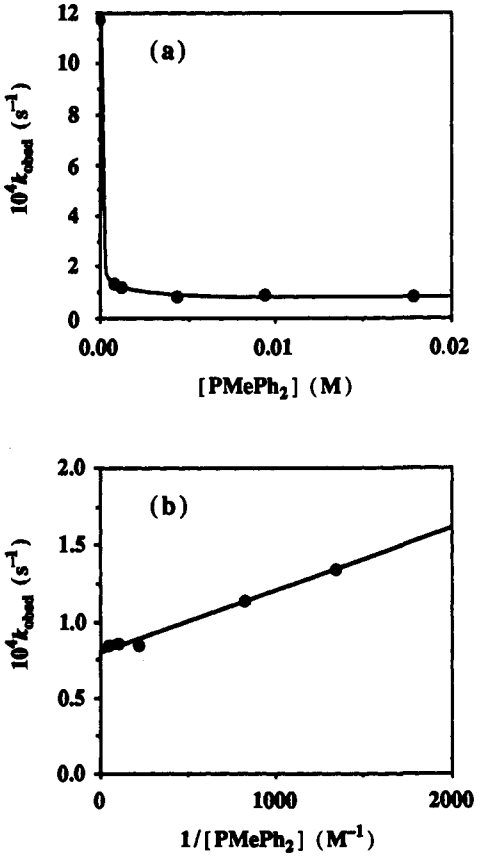

Figure 3. Effect of added $PMePh_2$ on the reductive elimination of *cis*-**2** in benzene-d_6 in the presence of diphenylacetylene at 40 °C. Initial concentration: [*cis*-**2**] = 0.015 M; [PhC≡CPh] = 0.15 M.

$PMePh_2$ (δ −27.2) appeared (Figure 2b). Of the signals in part b, the doublet at δ −3.1 (P(1')) ($^2J_{P-P}$ = 20 Hz, $^1J_{Pt-P}$ = 1382 Hz) involved satellites due to the coupling to the ^{29}Si nucleus ($^2J_{Si-P}$ = 195 Hz), indicating its trans orientation toward the silyl ligand. On the basis of the chemical shift, this signal is assigned to the PMe_2Ph ligand in **5**. On the other hand, the other doublet (P(2')) of almost the same chemical shift (δ 6.2, $^1J_{Pt-P}$ = 2138 Hz) as the P(2) signal of *cis*-**2** is assigned to the $PMePh_2$ ligand in **5**, that is trans to the methyl ligand. Thus it was clearly observed that the $PMePh_2$ ligand trans to the silyl ligand in *cis*-**2** is selectively replaced by PMe_2Ph.

Reductive Elimination Reactions. The *cis*- and *trans*-(silyl)(methyl) complexes (**2** and **3**, respectively) were readily decomposed in solution to yield $MeSiPh_3$ as the reductive elimination product in quantitative yields. The reaction of *trans*-**3** took place under heated conditions over 50 °C, whereas *cis*-**2** decomposed even at room temperature.

Kinetic examination was performed for the reductive elimination of *cis*-**2**. The thermolysis in benzene-d_6 in the presence of diphenylacetylene obeyed the first-order rate law in the concentration of *cis*-**2** over 70% conversion. Diphenylacetylene was added to trap the $[Pt(PMePh_2)_2]$ species generated in the reductive elimination as a stable $Pt(PhC{\equiv}CPh)(PMePh_2)_2$ complex (eq 1).[16]

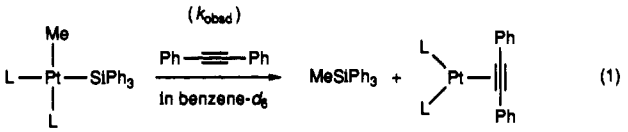

2: L = $PMePh_2$

Addition of free $PMePh_2$ to the system effectively retarded the reaction progress (Figure 3a). The plot of k_{obsd} vs $1/[PMePh_2]$ gave a straight line as shown in Figure 3b. On the other hand, the rate of reductive elimination increased linearly as the concentration of diphenylacetylene increased (Figure 4).[17] The

(16) In the absence of trapping agents such as diphenylacetylene, thermolysis of *cis*-**2** did not obey the first-order rate law probably because of the effect of coordinatively unsaturated platinum species.

(17) In the kinetic studies under the conditions with low concentration of diphenylacetylene ([PhC≡CPh] = 0.100 and 0.139 M), the effect of change in the acetylene concentration could not be ignored at later stages of the reaction. Therefore, the rate constants were obtained from the kinetic data at low conversion of *cis*-**2** (up to 17.5% conversion at 0.100 M; up to 32.4% conversion at 0.139 M). Under these conditions, the first-order plots exhibited good linear correlations (r = 0.997 for 11 data points at 0.100 M; r = 0.999 for 16 data points at 0.139 M).

(18) Kobayashi, T.; Hayashi, T.; Yamashita, H.; Tanaka, M. *Chem. Lett.* **1988**, 1411.

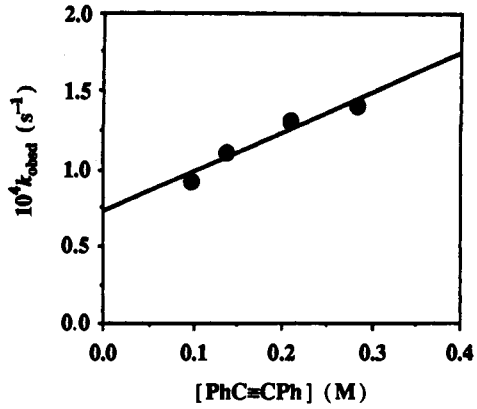

Figure 4. Effect of diphenylacetylene on the reductive elimination of *cis*-**2** in benzene-d_6 in the presence of $PMePh_2$ at 40 °C. Initial concentration: [*cis*-**2**] = 0.022 M; [$PMePh_2$] = 0.0020 M.

Table 2. Rate of Reductive Elimination of *cis*-**2** in Benzene-d_6 at 30 °C[a]

additive (M)	$10^4 k_{obsd}$ (s^{-1})
$MeO_2CC{\equiv}CCO_2Me$	very fast (23×10^{-4} s^{-1} at 10 °C)[b]
PhC≡CPh	3.9
maleic anhydride	>90 (6.6×10^{-4} s^{-1} at 10 °C)[b]
dimethyl maleate	1.8
trans-stilbene	1.6
styrene	1.0

[a] The rate constant was measured in benzene-d_6 at 30 °C in the presence of 0.137 M additive. Initial concentration: [*cis*-**2**] = 0.015 M. [b] Rate constant measured at 10 °C.

Scheme 3

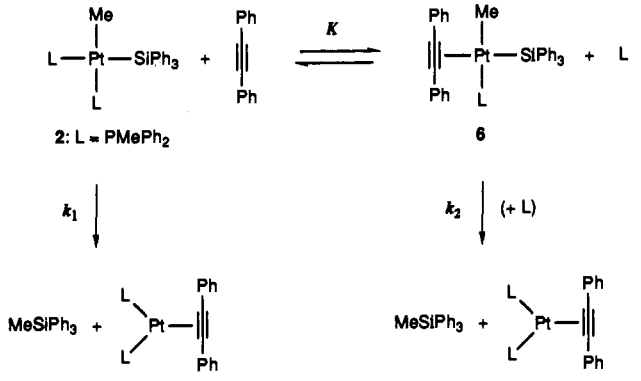

rate constants in Figure 4 were measured in the presence of a constant concentration of free $PMePh_2$ (vide infra).

The reductive elimination rates of *cis*-**2** were measured at four different temperatures (10, 20, 30, and 35 °C) in benzene-d_6 in the presence of diphenylacetylene (0.035 M), and the following activation parameters were estimated: $E_a = 24.9 \pm 0.5$ kcal mol^{-1}, $\Delta S^{\ddagger} = 4.3 \pm 1.0$ eu, $\Delta G^{\ddagger} = 22.9 \pm 0.5$ kcal mol^{-1} at 313 K.

Table 2 lists the rates of reductive elimination of *cis*-**2** in the presence of a variety of olefins and acetylene derivatives. It is seen that acetylenes and olefins with electron-withdrawing group(s) effectively enhance the reductive elimination. Particularly, in the presence of dimethyl acetylenedicarboxylate and maleic anhydride, instant formation of $MeSiPh_3$ was observed at 30 °C.

Mechanism of Reductive Elimination of *cis*-2. The *cis*-(silyl)(methyl)platinum complex **2** readily underwent the reductive elimination of $MeSiPh_3$ under mild conditions. The kinetic results suggest the reaction mechanism depicted in Scheme 3.

The methylsilane formation predominantly proceeds from a monophosphine intermediate **6**, which is formed by ligand displacement of one of the $PMePh_2$ ligands in *cis*-**2** with diphenylacetylene. The coordination of diphenylacetylene must take place at the site trans to the silyl ligand because of the greater trans effect of the silyl ligand than the methyl ligand. The fact that the reductive elimination still proceeds at high concentration of free $PMePh_2$ (Figure 3) indicates the minor reductive elimination pathway without dissociation of the $PMePh_2$ ligand. Assumption of a rapid equilibration between *cis*-**2** and **6** leads to the kinetic expression in eq 2 where $[PtMe(SiPh_3)]_{total}$ is the sum of the concentrations [*cis*-**2**] and [**6**] at time t.

$$\frac{d[MeSiPh_3]}{dt} = \frac{k_1 + \dfrac{k_2K[PhC{\equiv}CPh]}{[L]}}{1 + \dfrac{K[PhC{\equiv}CPh]}{[L]}}[PtMe(SiPh_3)]_{total} \quad (2)$$

If the relation $K[PhC{\equiv}CPh]/[L] = [\mathbf{6}]/[cis\text{-}\mathbf{2}] \ll 1$ holds and the concentration of free $PMePh_2$ ([L]) is assumed to be constant during the reaction when free $PMePh_2$ was added, k_{obsd} can be expressed by eq 3.

$$k_{obsd} = k_1 + \frac{k_2K[PhC{\equiv}CPh]}{[L]} \quad (3)$$

Equation 3 is consistent with the experimental results represented by Figures 3 and 4. Thus the values of intercepts in Figures 3b and 4, which correspond to the reductive elimination rate without dissociation of $PMePh_2$ (k_1), were in fair agreement with each other (0.79×10^{-4} s^{-1}). Furthermore, the k_2K value (2.7×10^{-3} s^{-1}) derived by dividing the slope of the straight line in Figure 3b by the concentration of diphenylacetylene was in agreement with the value of 3.0×10^{-3} s^{-1} that was obtained by multipling the slope of the straight line in Figure 4 by the concentration of $PMePh_2$ added to the system.

Conclusion

We succeeded for the first time in measuring the rate of reductive elimination of an isolated silyl–methyl complex *cis*-**2**. It is noteworthy that the reductive elimination of the silyl–methyl complex is much faster than those of the related *cis*-bis(silyl)platinum and *cis*-dimethylplatinum complexes bearing two $PMePh_2$ ligands (*cis*-Pt($SiMe_2Ph$)$_2$($PMePh_2$)$_2$[18,19] and *cis*-$PtMe_2$($PMePh_2$)$_2$[5]). Further studies focusing on the catalytic mechanism of hydrosilylation are now in progress.

Experimental Section

General Procedure and Materials. All manipulations were carried out under a nitrogen atmosphere using conventional Schlenk techniques. Nitrogen gas was dried by passage through P_2O_5 (Merck, SICAPENT). NMR spectra were recorded on a JEOL JNM-EX270 spectrometer (^{1}H, 270.05 MHz; ^{31}P NMR, 109.25 MHz). Chemical shifts are reported in δ ppm referenced to an internal $SiMe_4$ standard for ^{1}H NMR and to an external 85% H_3PO_4 standard for ^{31}P NMR. Elemental analyses were performed by the Hokkaido University Analytical Center.

THF and Et_2O were dried over sodium benzophenone ketyl and distilled just before use. CH_2Cl_2 was dried over CaH_2 and distilled just before use. Benzene-d_6 was dried over $LiAlH_4$ and vacuum transferred and stored under a nitrogen atmosphere. $PMePh_2$ and PMe_2Ph were prepared by the reactions of MeMgBr with $PClPh_2$ and PCl_2Ph, respectively. Me_2SiPh_2 was prepared by treatment of Ph_2SiCl_2 with MeMgBr. *trans*-$PtCl(SiPh_3)(PMePh_2)_2$ (**1**) was prepared as reported.[10] All other compounds used in this study were obtained from commercial sources and used without further purification.

Preparation of *cis*-PtMe($SiPh_3$)($PMePh_2$)$_2$·Et_2O (2). To a solution of *trans*-$PtCl(SiPh_3)(PMePh_2)_2$ (303 mg, 0.34 mmol) in THF (8 mL) was added an ether solution of MeLi (1.4 M, 0.6 mL, 0.84 mmol) at 0 °C. The mixture was stirred at room temperature for 30 min and then cooled to −20 °C. Methanol (0.5 mL) was slowly added, and the solution was concentrated to dryness. The resulting yellow-orange solid was

(19) It was confirmed that *cis*-Pt($SiPh_3$)$_2$($PMePh_2$)$_2$ is much more stable than *cis*-**2** toward reductive elimination: $k_{obsd} = 0.57 \times 10^{-4}$ s^{-1} at 60 °C in benzene in the presence of diphenylacetylene (0.137 M).

Table 3. Crystal Data and Details of the Structure Determination for *cis*-PtMe(SiPh$_3$)(PMePh$_2$)$_2$·Et$_2$O (**2**)

formula	$C_{45}H_{44}P_2PtSi·C_4H_{10}O$
formula wt	944.09
habit	prismatic
cryst size, mm	0.15 × 0.3 × 0.4
cryst system	monoclinic
space group	$P2_1/c$ (No. 14)
a, Å	16.113(3)
b, Å	11.354(3)
c, Å	25.216(2)
β, deg	104.73(1)
V, Å^3	4461(1)
Z	4
d_{calcd}, g cm^{-3}	1.405
μ(Mo Kα), cm^{-1}	32.65
F(000)	1912
radiation	Mo Kα (λ = 0.710 69 Å)
monochromator	graphite
data collected	$+h,+k,\pm l$
2θ range, deg	5.0–45.0
scan type	ω
$\Delta\omega$, deg	0.83 + 0.35 tan θ
scan speed, deg min^{-1}	6, fixed
temp, K	296
linear decay, %	13.9
absorption correction	empirical
min and max transmission factors	0.683, 0.998
no. of reflections collected	6440
no. of unique reflections	6185 (R_{int} = 0.021)
no. of observed reflections	4534 ($I \geq 2\sigma(I)$)
no. of variables	487
R	0.038
R_w	0.033
goodness of fit	1.72
max Δ/σ in final cycle	0.002
max and min peak, e Å^{-3}	1.62, –0.92 (near Pt)

extracted with CH_2Cl_2 (2 × 5 mL), and the extract was filtered though a filter-paper-tipped cannula and concentrated to ca. 1 mL. Et_2O (ca. 5 mL) was carefully layered on the CH_2Cl_2 solution, and the solvent layers were allowed to stand at –20 °C to form colorless crystals of *cis*-**2** suitable for X-ray diffraction study (243 mg, 76%). The product contained 1 equiv of Et_2O in the crystal as confirmed by ^{1}H NMR spectroscopy. Anal. Calcd for $C_{45}H_{44}P_2PtSi·C_4H_{10}O$: C, 62.24; H, 5.45. Found: C, 62.04; H, 5.60. The NMR data are listed in Table 1.

Preparation of *trans*-PtMe(SiPh$_3$)(PMePh$_2$)$_2$·CH$_2$Cl$_2$ (3). To a solution of *trans*-PtCl(SiPh$_3$)(PMePh$_2$)$_2$ (271 mg, 0.30 mmol) in THF (8 mL) was added an ether solution of Me_2Mg (0.93 M, 0.8 mL, 0.74 mmol) at 0 °C. The mixture was stirred at room temperature for 30 min and then cooled to –20 °C. Methanol (0.5 mL) was slowly added, and the solution was concentrated to dryness. The resulting solid was extracted with CH_2Cl_2 (2 × 5 mL), and the extract was filtered through a filter-paper-tipped cannula and concentrated to dryness. The yellow-orange solid thus obtained was dissolved in THF (1 mL) and CH_2Cl_2 (2 drops) at –20 °C, and Et_2O (5 mL) was carefully layered on the solution. The solvent layers were allowed to mix slowly at –20 °C to give colorless crystals of *trans*-**3** (140 mg, 49%). The product contained 1 equiv of CH_2Cl_2 in the crystal as confirmed by ^{1}H NMR spectroscopy. Anal. Calcd for $C_{45}H_{44}P_2PtSi·CH_2Cl_2$: C, 57.86; H, 4.86. Found: C, 57.58; H, 4.92.

X-ray Diffraction Study of *cis*-PtMe(SiPh$_3$)(PMePh$_2$)$_2$·Et$_2$O (2). A single crystal of dimensions ca. 0.15 × 0.3 × 0.4 mm was sealed in a glass capillary tube. Intensity data were collected on a Rigaku AFC5R four-circle diffractometer. Unit cell dimensions were obtained from a least-squares treatment of the setting angles of 25 reflections in the range 25.0 < 2θ < 28.8°. The cell dimensions suggested a monoclinic cell and systematic absences in the diffractometer data indicated the space group $P2_1/c$ (No. 14). Diffraction data were collected at 23 °C in the range 5.0 < 2θ < 45.0° using the ω scan technique at a scan rate of 6° min^{-1} in omega. Three standard reflections, monitored at every 150 reflection measurements, showed a linear decay in the intensity by 13.9%. The data were corrected for Lorentz and polarization effects, decay, and absorption (empirical, based on azimuthal scans of three reflections). Of the 6185 unique reflections measured, 4534 were classed as observed ($I > 2\sigma(I)$) and these were used for the solution and refinement of the structure.

Table 4. Positional Parameters and Equivalent Isotropic Thermal Parameters for *cis*-PtMe(SiPh$_3$)(PMePh$_2$)$_2$·Et$_2$O (**2**)

atom	x	y	z	B_{eq}[a]
Pt	0.22318(2)	–0.01514(2)	0.20308(1)	3.553(7)
P(1)	0.0981(1)	–0.0732(2)	0.13688(8)	3.86(5)
P(2)	0.2869(1)	0.0892(2)	0.14626(8)	3.93(5)
Si	0.3335(1)	0.0251(2)	0.28373(8)	3.83(5)
C(1)	0.1662(4)	–0.0982(7)	0.2600(3)	4.4(2)
C(2)	0.3457(5)	–0.0945(7)	0.3384(3)	4.0(2)
C(3)	0.3729(5)	–0.2059(8)	0.3270(3)	5.1(2)
C(4)	0.3787(6)	–0.2990(7)	0.3626(4)	5.6(3)
C(5)	0.3576(6)	–0.2851(8)	0.4115(3)	5.3(3)
C(6)	0.3319(6)	–0.1770(9)	0.4246(3)	5.8(3)
C(7)	0.3243(5)	–0.0811(7)	0.3883(3)	4.7(2)
C(8)	0.3076(5)	0.1685(7)	0.3151(3)	4.2(2)
C(9)	0.2419(6)	0.2396(7)	0.2863(3)	5.4(2)
C(10)	0.2184(6)	0.3448(8)	0.3061(4)	6.6(3)
C(11)	0.2632(8)	0.3814(9)	0.3580(5)	7.6(4)
C(12)	0.3272(7)	0.3138(9)	0.3887(4)	7.4(3)
C(13)	0.3497(6)	0.2086(8)	0.3671(4)	5.8(3)
C(14)	0.4482(5)	0.0348(6)	0.2757(3)	3.7(2)
C(15)	0.5088(5)	0.1181(7)	0.3022(3)	4.4(2)
C(16)	0.5910(6)	0.1187(8)	0.2963(3)	5.4(3)
C(17)	0.6163(5)	0.0366(9)	0.2630(4)	5.6(3)
C(18)	0.5593(6)	–0.0456(7)	0.2365(3)	5.4(2)
C(19)	0.4755(5)	–0.0465(6)	0.2427(3)	4.5(2)
C(20)	0.0966(5)	–0.0869(7)	0.0646(3)	4.8(2)
C(21)	0.0079(4)	0.0233(7)	0.1365(3)	4.0(2)
C(22)	–0.0605(5)	0.0398(7)	0.0907(3)	4.8(2)
C(23)	–0.1249(6)	0.1185(9)	0.0917(4)	5.9(3)
C(24)	–0.1240(6)	0.1818(8)	0.1376(4)	6.6(3)
C(25)	–0.0575(7)	0.1670(9)	0.1838(4)	7.1(3)
C(26)	0.0078(5)	0.0898(8)	0.1826(3)	5.6(2)
C(27)	0.0610(5)	–0.2215(7)	0.1489(3)	4.1(2)
C(28)	–0.0231(6)	–0.2472(8)	0.1495(3)	5.1(2)
C(29)	–0.0464(7)	–0.362(1)	0.1572(4)	6.8(3)
C(30)	0.0118(9)	–0.4505(9)	0.1631(4)	7.6(3)
C(31)	0.0948(8)	–0.4274(9)	0.1639(5)	8.0(4)
C(32)	0.1195(6)	–0.3120(8)	0.1569(4)	6.5(3)
C(33)	0.3548(5)	0.2141(7)	0.1736(3)	5.4(2)
C(34)	0.2099(5)	0.1656(7)	0.0899(3)	4.3(2)
C(35)	0.1428(6)	0.2258(7)	0.1019(3)	5.3(2)
C(36)	0.0823(6)	0.2843(8)	0.0610(4)	6.4(3)
C(37)	0.0915(7)	0.2815(9)	0.0080(4)	7.0(3)
C(38)	0.1573(7)	0.2227(9)	–0.0048(4)	6.4(3)
C(39)	0.2173(5)	0.1635(7)	0.0359(3)	5.1(2)
C(40)	0.3511(4)	0.0025(7)	0.1108(3)	4.0(2)
C(41)	0.4177(6)	0.0477(8)	0.0908(4)	6.0(3)
C(42)	0.4640(6)	–0.022(1)	0.0643(4)	6.7(3)
C(43)	0.4445(6)	–0.138(1)	0.0554(3)	6.2(3)
C(44)	0.3800(6)	–0.1851(7)	0.0747(3)	5.5(3)
C(45)	0.3335(5)	–0.1174(7)	0.1024(3)	4.7(2)
O	0.6943(8)	0.0239(8)	0.4654(4)	12.0(3)
C(46)	0.835(1)	0.088(1)	0.485(1)	17.0(8)
C(47)	0.764(1)	0.028(2)	0.4465(7)	14.2(7)
C(48)	0.629(1)	–0.047(1)	0.4376(6)	14.3(7)
C(49)	0.574(1)	–0.086(2)	0.4633(8)	19.6(9)

[a] $B_{eq} = (8\pi^2/3)\sum_i\sum_j[U_{ij}(a_i^*a_j^*)(\mathbf{a}_i\cdot\mathbf{a}_j)] = (4/3)\sum_i\sum_j[\beta_{ij}(\mathbf{a}_i\cdot\mathbf{a}_j)]$.

All calculations were performed with the TEXSAN Crystal Structure Analysis Package provided by Rigaku Corp., Tokyo, Japan.[20] The scattering factors were taken from International Tables for X-ray Crystallography.[21] The structure was solved by heavy atom Patterson methods (PATTY) and expanded using Fourier techniques (DIRDIF92). The structure was refined by full-matrix least-squares with anisotropic thermal parameters for all non-hydrogen atoms. In the final cycles of refinement, hydrogen atoms with isotropic temperature factors (B_{iso} = 1.20$B_{bonded\ atom}$) were located at idealized positions (d(C–H) = 0.95 Å) and were included in the calculation without refinement of their parameters. The function minimized in least-squares was $\Sigma w(|F_o|-|F_c|)^2$ ($w = 1/[\sigma^2(F_o)]$). The final R index was 0.038 (R_w = 0.033, S = 1.72). $R = \Sigma||F_o|-|F_c||/\Sigma|F_o|$ and $R_w = [\Sigma w(|F_o|-|F_c|)^2/\Sigma w|F_o|^2]^{1/2}$. $S = [\Sigma w(|F_o| - |F_c|)^2/(N_o - N_p)]^{1/2}$, where N_o is the number of observed data and N_p is the number of parameters varied. Crystal data and details of data

(20) TEXSAN Structure Analysis Package, Molecular Structure Corp., 1985 and 1992.

(21) Cromer, D. T.; Waber, J. T. *International Tables for X-ray Crystallography*; The Kynoch Press; Birmingham, U. K., 1974; Vol. IV.

collection and refinement are summarized in Table 3. Positional parameters for all non-hydrogen atoms are listed in Table 4. The atomic numbering scheme, positional parameters for hydrogen atoms, anisotropic thermal parameters, and bond distances and angles are reported in the supplementary material.

Reaction of *cis*-2 with PMe$_2$Ph. *cis*-PtMe(SiPh$_3$)(PMePh$_2$)$_2$·Et$_2$O (**2**) (20.7 mg, 21.9 μmol) was placed in an NMR sample tube equipped with a rubber septum cap and the system was replaced with nitrogen gas at room temperature. The sample tube was cooled to −20 °C, and CD_2Cl_2 (0.7 mL) and PMe_2Ph (4.40 mg, 31.8 μmol) were succesively added. The sample was placed in an NMR sample probe controlled to −20.0 ± 0.1 °C and examined by NMR spectroscopy. The NMR data for PtMe(SiPh$_3$)(PMe$_2$Ph)(PMePh$_2$) (**5**) are as follows. ^{1}H NMR (CD_2Cl_2, −50°C): δ 0.28 (dd, $^3J_{H-P}$ = 12.6 and 6.3 Hz, $^2J_{H-Pt}$ = 58.4 Hz, 3H, PtCH_3), 1.09 (d, $^2J_{H-P}$ = 7.6 Hz, $^3J_{H-Pt}$ = 15.2 Hz, 6H, P(CH_3)$_2$Ph), 1.35 (d, $^2J_{H-P}$ = 8.2 Hz, $^3J_{H-Pt}$ = 28.4 Hz, 3H, P(CH_3)Ph$_2$), 7.0–7.7 (m, *Ar*). ^{31}P{^{1}H} NMR (CD_2Cl_2, 20°C): δ 6.2 (d, $^2J_{P-P}$ = 20 Hz, $^1J_{P-Pt}$ = 2138 Hz), −3.1 (d, $^2J_{P-P}$ = 20 Hz, $^1J_{P-Pt}$ = 1382 Hz, $^2J_{P-Si}$ = 195 Hz).

Kinetic Studies. A typical procedure for measuring the rate of reductive elimination of *cis*-**2** is as follows. *cis*-PtMe(SiPh$_3$)(PMePh$_2$)$_2$ (**2**) (9.59 mg, 10.2 μmol), $PMePh_2$ (1.31 mg, 6.52 μmol), and Me_2SiPh_2 (0.97 mg, 4.6 μmol) as an internal reference were placed in an NMR sample tube equipped with a rubber septum cap and the system was replaced with nitrogen gas at room temperature. The sample tube was cooled to −20 °C and a stock solution of diphenylacetylene in benzene-d_6 (0.150 M, 0.70 mL) was added. The sample was placed in an NMR sample probe controlled to 30.0 ± 0.1 °C and examined by ^{1}H NMR spectroscopy. The amount of $MeSiPh_3$ produced with time was determined by measuring the relative peak integration of the methyl signals of $MeSiPh_3$ (δ 0.73) and Me_2SiPh_2 (δ 0.45).

Acknowledgment. This work was supported by the Grant-in-Aid for Scientific Research on Priority Area of Reactive Organometallics No. 05236106 from the Ministry of Education, Science and Culture, Japan. Partial financial support from Asahi Glass Foundation is gratefully acknowledged.

Supplementary Material Available: ^{31}P{^{1}H} NMR spectra showing the sequence of reactions (**1** → **4** → **2**), atomic numbering scheme for *cis*-**2**·Et$_2$O, and tables of hydrogen atom positional parameters, anisotropic thermal parameters, and bond distances and angles for *cis*-**2**·Et$_2$O (9 pages); listing of observed and calculated structure factors for *cis*-**2**·Et$_2$O (31 pages). This material is contained in many libraries on microfiche, immediately follows this article in the microfilm version of the journal, and can be ordered from the ACS; see any current masthead page for ordering information.